Multifrequency Reconstruction of Moderately Rough Interfaces via Quasi-Ray Gaussian Beams

Vincenzo Galdi, *Member, IEEE*, David A. Castañon, *Senior Member, IEEE*, and Leopold B. Felsen, *Life Fellow, IEEE*

***Abstract*—In this paper, we present a new technique for determining the surface profile of a moderately rough interface between air and a homogeneous dielectric half-space. Based on sparsely sampled step-frequency ground penetrating radar measurements, the proposed inversion scheme uses a quasi-ray Gaussian beam fast forward model, coupled with a low-order parameterization of the surface profile in terms of B-splines. The profile estimation problem is posed as a parameter optimization problem, which is solved using a multiresolution continuation method via *frequency hopping*. Numerical experiments establish that the algorithm is efficient and yields accurate reconstructions throughout most of the illuminated region even in noisy environments, losing accuracy only in regions with very weak illumination.**

***Index Terms*—Gaussian beams, ground penetrating radars, inverse scattering, rough surfaces.**

I. Introduction

THE problem of determining the properties of rough surfaces from electromagnetic (EM) reflected field data arises in many important applications, ranging from nondestructive testing to underground imaging. In this paper, we address underground imaging via ground-penetrating radar (GPR). In GPR systems, arrays of above-ground transmitters and receivers illuminate areas of interest and receive backscattered signals from underground objects and from surface reflections. The shape of the air-ground interface is unknown and constitutes a principal corruptor of the backscattered signal from subsurface targets of interest. In order to enhance subsequent detection, classification and inverse scattering processing, it is important to compensate for the distortion introduced by the air-ground interface.

One possible approach for this compensation is to characterize the statistics of the distortion caused by unknown rough surfaces and then apply appropriate statistical signal processing techniques. Such an approach was used in [1]–[4] for detection of buried mines via both forward-looking and downward-looking GPR systems. However, this approach fails to exploit deterministic information present in the received signals due to scattering from the air-ground interface and thus yields limited accuracy and robustness in classification and reconstruction (see, e.g., [5]). In this paper, we address the problem of estimating the profile of the air-ground interface from in-situ frequency-stepped GPR measurements, for use in subsequent imaging and classification processing.

Estimation of rough surfaces from inverse scattering has received considerable attention in the past decade. However, most of the available algorithms have focused on conducting surfaces. Wombell and DeSanto [6], [7] used Kirchhoff approximation and Fourier transform to estimate surface profiles based on measurements of the reflected field in all spectral directions. Noguchi and his colleagues [8], [9] used nonlinear optimization techniques for direct estimation of surfaces illuminated by monochromatic Gaussian beams, based on the far-field scattering amplitude for all spectral directions. In a different approach, Schatzberg and Devaney [10] used Rytov approximation and backpropagation to estimate surface profiles based on full measurements of the reflected wave.

In contrast with the above contributions, our work in this paper is focused on estimating surface profiles based on reflection from a moderately rough interface between air and a homogeneous dielectric half-space (soil), as illustrated in Fig. 1. Furthermore, we assume that the reflected field is measured only at receivers with discrete spatial locations, using a stepped-frequency GPR. We assume that the incident field arises from a discrete set of transmitters and thus has a finite aperture.

First we employ a forward model relating the measured fields at the receivers to the surface profile. This model, detailed in [11], utilizes Gabor-based Gaussian beam algorithms in conjunction with the complex source point (CSP) method for generating beam-like wave objects [12]–[14]. With this model, together with a parametric representation of the surface in terms of B-splines [15], the surface estimation problem is posed as a nonlinear optimization problem, similar in spirit to the approach in [8]. We show that this optimization problem has local minima and exploit a multiresolution continuation strategy based on *frequency hopping* [16]–[18], to approach convergence to globally optimal estimates of surface profiles.

The rest of this paper is organized as follows: Section II describes the problem of rough surface reconstruction from frequency-stepped GPR measurements and poses the estimation problem as a nonlinear optimization problem. Section III describes the surface parameterization, the Gabor-based Gaussian

Manuscript received September 8, 2000; revised June 12, 2001. This work was supported by ODDR&E under MURI Grants ARO DAAG55-97-1-0013 and AFOSR F49620-96-1-0028 and by the Engineering Research Centers Program of the National Science Foundation under Award EEC-9986821. The work of V. Galdi was also supported by a European Union postdoctoral fellowship through the University of Sannio, Benevento, Italy. L. B. Felsen was supported in part by Grant 9900448 by the U.S.-Israel Binational Science Foundation, Jerusalem, Israel, and from Polytechnic University, Brooklyn, NY.

V. Galdi is with the Department of Electrical and Computer Engineering, Boston University, Boston, MA 02215 USA, on leave from University of Sannio, Benevento, Italy (e-mail: vgaldi@bu.edu).

D. A. Castañon is with the Department of Electrical and Computer Engineering, Boston University, Boston, MA 02215, USA (e-mail: dac@bu.edu).

L. B. Felsen is with the Department of Aerospace and Mechanical Engineering and the Department of Electrical and Computer Engineering, Boston University, Boston, MA 02215, USA and also with the Polytechnic University, Brooklyn, NY 11201 USA (e-mail: lfelsen@bu.edu).

Publisher Item Identifier S 0196-2892(02)01882-X.

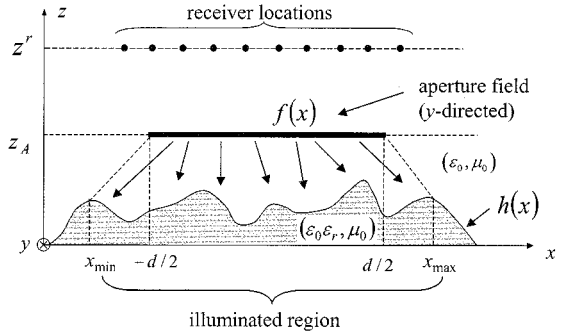

Fig. 1. Setup geometry for the inverse scattering problem. An aperture-excited, time-harmonic, TM-polarized EM field illuminates a homogeneous dielectric half-space with known relative permittivity ϵ_r and with a moderately rough interface whose coarse scale profile is described by the continuous function $h(x)$. The reflected field is sampled at N_r receiver locations at $z = z^r$.

beam algorithm, the multiresolution continuation algorithm and the resulting optimization approach for determining the surface profile. Section IV details the results of numerical experiments to illustrate the accuracy of the surface reconstructions under different conditions. Section V provides concluding remarks.

II. Statement of the Problem

The problem of interest is reconstructing the air-ground interface coarse-scale profile from a limited number of spatially sampled reflected field measurements, using a limited aperture illumination from a frequency-stepped GPR system. We consider a two-dimensional (2-D) model, as depicted in Fig. 1, where a TM-polarized EM field with implicit time-harmonic dependence $\exp(-i\omega t)$ illuminates a dielectric half-space with known relative permittivity ϵ_r and a moderately rough interface, whose coarse scale profile is described by a continuous function $h(x)$. The field is assumed to be generated by an extended aperture distribution at $z = z_A$,

$$\mathbf{E}^{inc}(x, z_A) = f(x)\mathbf{u}_y, \quad |x| \leq \frac{d}{2}, \quad z = z_A \tag{1}$$

where $\mathbf{u}_y$ denotes a y-directed unit vector.

In this preliminary investigation, we neglect the presence of any buried object; surface estimation strategies in the presence of shallowly buried plastic mine-like targets, not very different in principle, are dealt with elsewhere [19]–[22]. Furthermore, we also neglect the *noisy* (incoherent) contribution of finer-scale roughness and focus on estimation of the coarse shape, acknowledging the implicit limits of retrievable information through inverse scattering (see, e.g., [23] and the more relevant *near-proximity* extension [24]). The y-directed reflected electric field is sampled at a number N_r of fixed receiver locations $x_1^r, \ldots, x_{N_r}^r$ at the observation plane $z = z^r$. As common in many GPR systems, we assume to work in a *step-frequency* regime with N_λ different operating wavelengths (frequencies), so that a set of $N_r \times N_\lambda$ complex (magnitude and phase) samples constitutes the *observed data* of the problem. It is well-known that this inverse scattering problem is *ill-posed* and therefore a *blind* implementation of inverse scattering techniques would result in *ill-conditioned* numerical algorithms. We refer the interested reader to [23], [24] for analysis of the *retrievable information* from both theoretical and computational viewpoints.

Here, a *robust* inversion strategy via a well-posed inverse of the problem is achieved by

i) Introducing a finite-dimensional compact geometrical parameterization of the unknown interface profile;
ii) Estimating the unknown parameters by *fitting* the model-based forward scattering prediction to the available (measured/simulated) data, i.e., minimizing a suitable *cost functional*.

A key issue in this robust strategy is selection of an appropriate interface profile parameterization. This requires tradeoff between versatility, compactness and computational burden, bearing in mind that the number of unknown parameters to be estimated must be *smaller* than the collected reflected data size. Therefore, assuming that the collected data are *nonredundant* [23], [24], the maximum number of parameters that can be reliably estimated is $\sim N_r \times N_\lambda$. For the purposes of this paper, we assume that the surface shape can be approximated by a finite set of basis functions with unknown coefficients,

$$h(x) \approx \sum_{n=1}^{N} c_n s_n(x). \tag{2}$$

Let $\mathcal{E}_y^{refl}(x_p^r, \lambda_q)$ denote the complex reflected field *measured* at wavelength λ_q at receiver location x_p^r. Let $\underline{c}$ denote the vector of coefficients $c_n, n = 1, \ldots, N$. Given a vector of coefficients $\underline{c}$ and the outgoing field from the aperture distribution in (1), we can use the Gabor-based Gaussian beam algorithm in [11] (see also Section III-B) for the surface profile in (2) to generate predictions of the reflected field at each receiver. Let $E_y^{refl}(x_p^r, \lambda_q; \underline{c})$ denote the complex reflected field *predicted* from $\underline{c}$ at (free-space) wavelength λ_q at receiver location x_p^r. With this notation, we define the weighted approximation error $J(\underline{c})$ as follows:

$$\begin{aligned} J(\underline{c}) &= \left\| \underline{E}^{refl}(\underline{c}) - \underline{\mathcal{E}}^{refl} \right\|^2 \\ &= \sum_{p=1}^{N_r} \sum_{q=1}^{N_\lambda} \alpha_{pq} \left| E_y^{refl}(x_p^r, \lambda_q; \underline{c}) \right. \\ &\qquad \left. - \mathcal{E}_y^{refl}(x_p^r, \lambda_q) \right|^2, \end{aligned} \tag{3}$$

for receiver locations $x_1^r, \ldots, x_{N_r}^r$ and operating wavelengths $\lambda_1, \ldots, \lambda_{N_\lambda}$, $\alpha_{pq} > 0$ being (arbitrary) weight coefficients.

The regularized inverse scattering problem can now be formalized as finding the coefficient vector $\underline{c}$ in (2) which minimizes the cost functional (3), i.e., finding $\hat{\underline{c}}$ such that

$$\hat{\underline{c}} = \arg\min_{\underline{c}} J(\underline{c}) \tag{4}$$

In general, the predictive model $E_y^{refl}(x_p^r, \lambda_q; \underline{c})$ is a highly nonlinear function of the coefficients $\underline{c}$. Thus, the resulting minimization problem may have multiple local minima. In the next section, we describe the choice of basis functions used in our representation, the forward scattering model and the optimization approach used for determining global minima of the cost functional (3).

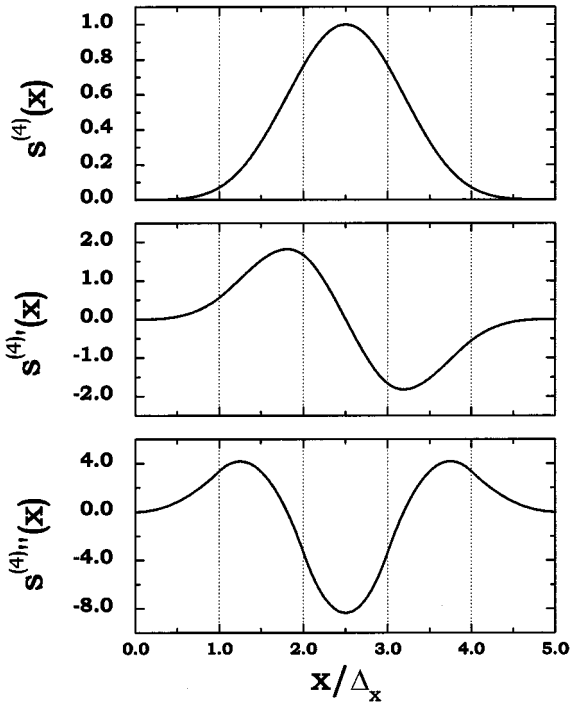

Fig. 2. Quartic B-spline basis function and its first two derivatives. $'$ denotes (d/dx).

III. Algorithmic Aspects

A. Interface Profile Parameterization

As our choice of basis functions in (2), we used shifted B-splines [15] selected with a fixed resolution matched to the coarse level of detail for the reconstruction. In particular, we chose a quartic-spline basis function $s^{(4)}(x)$, where (5), shown at the bottom of the page, and $X = x/\Delta_x$. This basis function has finite support and differentiable second derivatives (see Fig. 2). The surface profile is thus approximated as a linear combination of shifted B-spline basis functions,

$$h(x) \approx \sum_{n=-4}^{N_h-1} c_n s^{(4)}(x - x_n), \quad x_{\min} \le x \le x_{\max}, \quad (6)$$

$$x_n = x_{\min} + n\Delta_x, \quad \Delta_x = \frac{x_{\max} - x_{\min}}{N_h}. \quad (7)$$

The resulting linear combination (6) is a triply differentiable function with $N_h + 4$ degrees of freedom. We tried using cubic splines, but did not obtain satisfactory accuracy for the forward (beam) solver. We can speculate that the differentiability of the *second* derivative (and hence of the radius of curvature) is required by the beam algorithm. In this investigation, we assume *a priori* knowledge of the scale parameter Δ_x in (6) (i.e., the number of B-spline basis functions) and focus on retrieving the unknown coefficients c_n only. A more general *adaptive* framework is presented in [25].

B. The Gabor-Based Gaussian Beam Algorithm

The forward scattering predictive model is detailed in [11]. It is based on a recently developed Gabor-based narrow-waisted Gaussian beam (NW-GB) algorithm for reflection from and transmission through, moderately rough dielectric interfaces. The main steps of the algorithm can be summarized as follows:

1) The aperture field distribution in (1) is discretized self-consistently via Gabor expansion in terms of *narrow* Gaussian basis functions, which generate narrow-waisted *ray-like* Gaussian beams (GBs) launched from points on the aperture.
2) Each individual GB interaction with the rough interface is tracked via the complex-source-point (CSP) paraxial scheme (*quasi-reel* ray tracing) developed in [14] for circular cylindrical dielectric layers and generalized in [11] to rough surface geometries.
3) The various reflected/transmitted GB contributions are recombined at the observer.

In [11], the NW-GB algorithm has been validated and calibrated against an independently generated rigorous numerical solution [26] and has been shown to provide accurate and robust predictions over a range of calibrated combinations of the problem parameters, including moderate roughness with maximum slopes $\lesssim 40^\circ$, (average) curvature radii R_c larger than a wavelength, incidence directions far from grazing (incidence angles $\lesssim 30^\circ$ relative to z) and dielectric contrasts with $\mathrm{Re}(\epsilon_r)$ ranging from 1.2 to 10 and $\mathrm{Im}(\epsilon_r)$ up to 0.5. Though based on high-frequency asymptotics, the algorithm was found to provide satisfactory accuracy even for relatively *low-frequency* geometries ($R_c \sim 0.5\lambda$) and near-zone observation distances ($z^r \sim \lambda$). We refer the interested reader to [11] for theoretical and computational details and to [27] for extension to pulsed excitation.

As noted earlier, the computational feasibility of the proposed nonlinear inverse scattering algorithm is strongly tied to the efficiency of the forward solver. In this connection, full-wave techniques are most likely not affordable in terms of computing time and resources. Conversely, NW-GB algorithms, though not suffering from failures near caustics and other ray-field transition regions, preserve the attractive computational features of standard ray methods in the presence of large computational domains, with minimal memory requirements and typical computing times (for a field sample at a single position) of about 5–10 ms on a 500 MHz PC, which are fairly shorter than those

$$s^{(4)}(X) = \begin{cases} \frac{8}{115}X^4, & 0 \le X < 1, \\ -\frac{8}{115}\left(5 - 20X + 30X^2 - 20X^3 + 4X^4\right), & 1 \le X < 2, \\ \frac{8}{115}\left(155 - 300X + 210X^2 - 60X^3 + 6X^4\right), & 2 \le X < 3 \\ -\frac{8}{115}\left(655 - 780X + 330X^2 - 60X^3 + 4X^4\right), & 3 \le X < 4, \\ \frac{8}{115}(X-5)^4, & 4 \le X < 5 \end{cases} \quad (5)$$

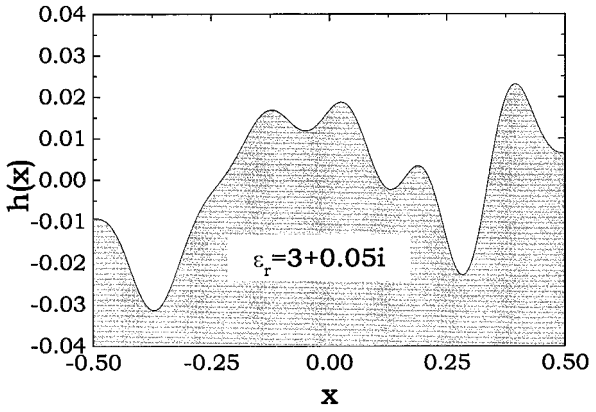

Fig. 3. Interface profile and simulation parameters (in arbitrary units) for the synthetic experiment discussed in Section III-C. Spline parameters: $N_h = 12$, $\Delta_x = 1/12$, $x_{\min} = -0.5$, $x_{\max} = 0.5$, maximum slope $\phi_{\max} = 34°$; aperture parameters (nonphased cosine distribution (8)): $d = 0.8$, $z_A = 0.6$; observation points: $N_r = 10$, $z^r = 0.6$, $x_p^r = -0.5 + (p-1)/(N_r - 1)$, $p = 1, \ldots, N_r$; operating wavelengths: $N_\lambda = 4$, $\lambda_1 = 0.2$, $\lambda_2 = 0.1$, $\lambda_3 = 0.067$, $\lambda_4 = 0.05$; weight coefficients: $\alpha_{pq} = 1 \; \forall \, p, q$. Relative permittivity: $\epsilon_r = 3 + 0.05i$.

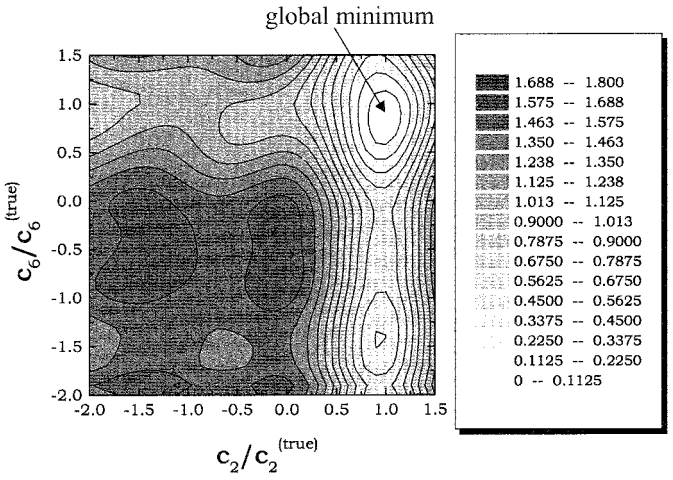

Fig. 4. Parameters as in Fig. 3. Reduced 2-D cost functional (3) as a function of c_2 and c_6 scaled to their true values $c_2^{(true)}$, $c_6^{(true)}$. The remaining coefficients are set to their true value.

typical of full-wave techniques. Application of GB algorithms to inverse scattering scenarios was also suggested in [28], where they were found to provide a good tradeoff between accuracy and computational burden.

C. Optimization Strategy

As discussed in Section II, we want a vector of coefficients $\underline{c}$ to minimize the weighted error functional (3). As stated previously, this minimization is nontrivial since the cost functional in (3) is likely nonconvex with respect to $\underline{c}$; therefore, unless an accurate initial guess is available, standard descent-based optimization algorithms [29] are likely to end in local minima, which correspond to *spurious* solutions. To illustrate this issue, we considered a simplified experiment where all unknown coefficients were set to their true value, with the exception of two that are left variable. The resulting cost function has two degrees of freedom and can be easily displayed. The interface profile and experiment parameters are shown in Fig. 3. A nonphased cosine tapered aperture illumination

$$f(x) = \begin{cases} \cos\left(\frac{\pi x}{d}\right) & |x| \leq \frac{d}{2}, \\ 0, & |x| > \frac{d}{2} \end{cases} \tag{8}$$

was assumed, with the aperture width d chosen so as to irradiate the region of interest while avoiding edge effects.

In this example, the surface profile was generated randomly by using 16 B-spline basis functions ($N_h = 12$). We chose c_2 and c_6 as unknown and set the remaining 14 coefficients to their true value. Fig. 4 shows the resulting 2-D cost function, as a function of c_2 and c_6 scaled with respect to their true values $c_2^{(true)}$, $c_6^{(true)}$, respectively. As the figure illustrates, the cost function has a deep *global* minimum at $(c_2, c_6) \approx (c_2^{(true)}, c_6^{(true)})$, but also has a number of *local* minima. This behavior was verified for multiple choices of weight coefficients α_{pq}, thus confirming that standard descent optimization techniques (e.g., conjugate gradient [29]) may end up in local minima and that some technique for global optimization is needed. However, popular global optimizers

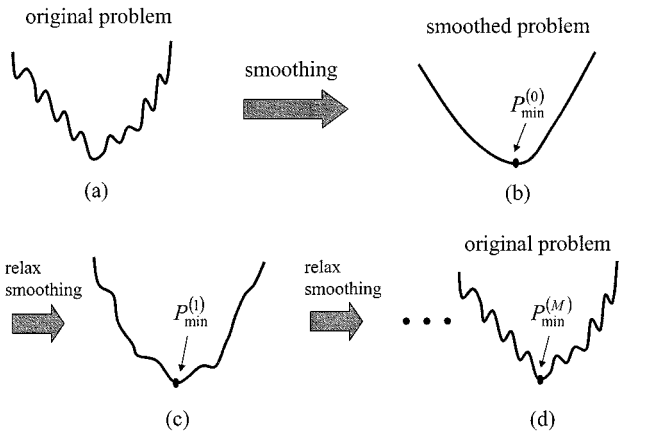

Fig. 5. Basic underlying scheme for continuation methods. (a): Original problem; (b): Local minima are filtered out through a smoothing procedure and a first rough estimate $P_{\min}^{(0)}$ of the global minimum is obtained via a standard descent optimizer; (c): The smoothing is partially relaxed and a refined estimate $P_{\min}^{(1)}$ is obtained using $P_{\min}^{(0)}$ as initial guess; (d): The smoothing is gradually removed in M iterations, restoring the original problem and obtaining the final estimate $P_{\min}^{(M)}$.

based on stochastic frameworks such as simulated annealing [30] and genetic algorithms [31] converge too slowly to be successfully exploited in realistic applications.

Our approach to finding global minima of (3) utilizes physics-based *multiresolution*, conceptually analogous to what in the optimization community is known as the *continuation method* [32]. The basic idea underlying continuation methods is illustrated in Fig. 5, with reference to a simple one-dimensional problem. Once a suitable smoothing parameter in the function to be minimized has been recognized, a smoothing procedure is applied in order to filter out the unwanted local minima. A standard descent minimization algorithm can be applied to the smoothed problem, yielding a rough estimation of the sought global minimum of the original problem. The smoothing is progressively relaxed, restoring the original problem and the solution is progressively refined, using at each stage a standard descent optimizer and exploiting as initial guess the estimation obtained at the previous stage.

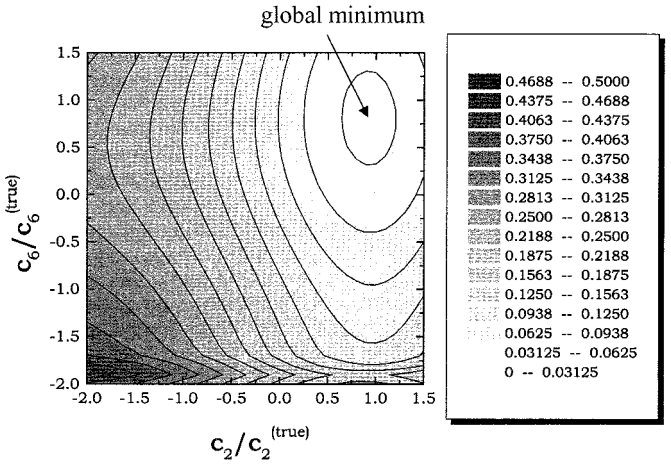

Fig. 6. Reduced 2-D cost functional as in Fig. 4, but using the longer wavelength ($\lambda_1 = 0.2$) data only.

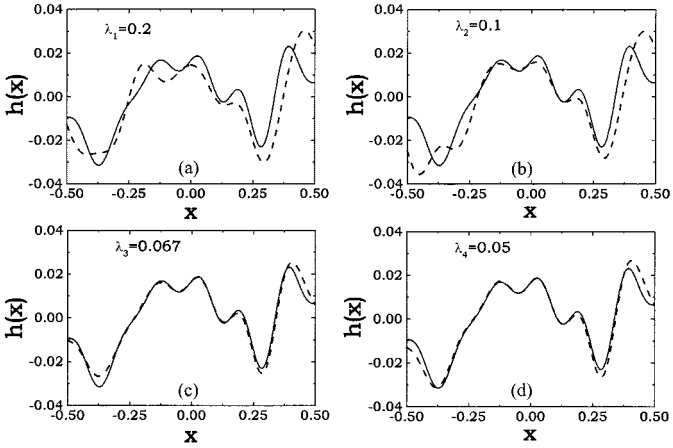

Fig. 7. Parameters as in Fig. 3. Convergence example for the proposed frequency-hopping strategy. (a): Reconstruction using only the $\lambda_1 = 0.2$ data and a flat interface ($c_n = 0, n = -4, \ldots, N_h - 1$) initial guess; (b), (c), (d): Refinements obtained using single-frequency data for $\lambda_2 = 0.1$, $\lambda_3 = 0.067$, $\lambda_4 = 0.05$, respectively and the previous stage reconstruction as initial guess. —— Actual profile; −−− Reconstruction.

As typical of many inverse scattering problems, the smoothness of the cost functional (3) strongly depends on the choice of operating wavelength(s). In particular, using larger wavelengths (i.e., lower frequencies) will result in a smoother functional. Furthermore, using lower frequencies reduces the possibility of phase ambiguity, one of the major causes of local minima. As an example, in Fig. 6 is shown the reduced 2-D cost function obtained using the same simulation parameters as in Fig. 4, but only the longer wavelength ($\lambda_1 = 0.2$) data. The resulting function is considerably smoother. The function still has a global minimum at $(c_2, c_6) \approx \left(c_2^{(true)}, c_6^{(true)}\right)$ with a large basin of attraction and *no* local minima. In this case, standard descent optimizers (e.g., conjugate gradient [29]) can be applied. The obtained estimate will need refining at other frequencies for two reasons: at lower frequencies, *i)* a *poorer* resolution can be expected and *ii)* the accuracy of the beam forward solver is *poorer* [11]. Nonetheless, this first estimate provides a good initial guess that can be further refined through progressively introducing the higher-frequency information into the optimization, in the spirit of the continuation method [32]. The proposed multiresolution strategy can be thus viewed as a continuation method, where the smoothing parameters are the weight coefficients α_{pq} associated with the different wavelengths. Among all possible ways of varying the weight coefficients α_{pq}, which corresponds to different ways of controlling the smoothing and the convergence behavior, we chose the simplest, i.e, an abrupt "on-off" variation. At each resolution stage, the frequency data to be included in the cost functional are selected by setting the corresponding weight coefficients α_{pq} to 0 or 1. This corresponds to what in the inverse scattering community is usually known as *frequency hopping* [16]–[18].

In our implementation, the partial optimization at each resolution level is performed using the Polak–Ribiere version of the conjugate gradient (CG) algorithm [29], particularly suited for nonquadratic functions. Specifically, the needed gradient of J is computed using a central difference formula, so that each gradient evaluation requires $2N_h + 8$ functional evaluations (i.e., $2N_h + 8$ solutions of a forward scattering problem), $N_h + 4$ being the number of unknown spline coefficients. The CG algorithm in [29] has been partially modified in order to enforce the consistency constraint

$$\max_x \{h(x)\} < z_A, z^r \tag{9}$$

where z_A and z^r are the aperture and observation heights, respectively (see Fig. 1).

IV. Numerical Results

In order to test our surface profile estimation algorithms, we generated synthetic field measurement data using a reliable full-wave solution of the forward scattering problem by means of the multifilament current method in [26], in conjunction with rigorous Kirchhoff aperture integration [33], for a variety of surfaces. For all numerical experiments presented below, the accuracy of the NW-GB forward solver was preliminarily verified. The simulation parameters are summarized in Fig. 3, with the dielectric half-space constitutive parameters chosen so as to simulate a class of sandy soils in the GPR frequency range. In this example, there are 16 unknown spline coefficients to be estimated, based on 40 complex (magnitude and phase) field samples. Reconstruction results are shown in Fig. 7. Assuming as initial guess a flat interface ($c_n = 0,\ n = -4, \ldots, N_h - 1$), the cost functional (3) was minimized using only the lowest frequency data ($\lambda_1 = 0.2$), obtaining the reconstruction shown in Fig. 7(a). Subsequent refinements of this reconstruction were obtained by including higher frequency data, resulting in the improved approximations shown in Fig. 7(b)–(d). Specifically, each iterative improvement in Fig. 7(b)–(d) is obtained by using only a *single frequency* at a time and exploiting the reconstruction at the previous (lower) frequency as initial guess. The more time-consuming alternative of using at each iteration the *current* frequency *plus* the lower ones was found not to yield significant improvement. The example illustrates that the reconstruction is accurate throughout most of the interval, except near the edges of the illuminated region; a similar phenomenon was observed in [8]. The likely explanation for this loss of accuracy is due to the weak illumination in

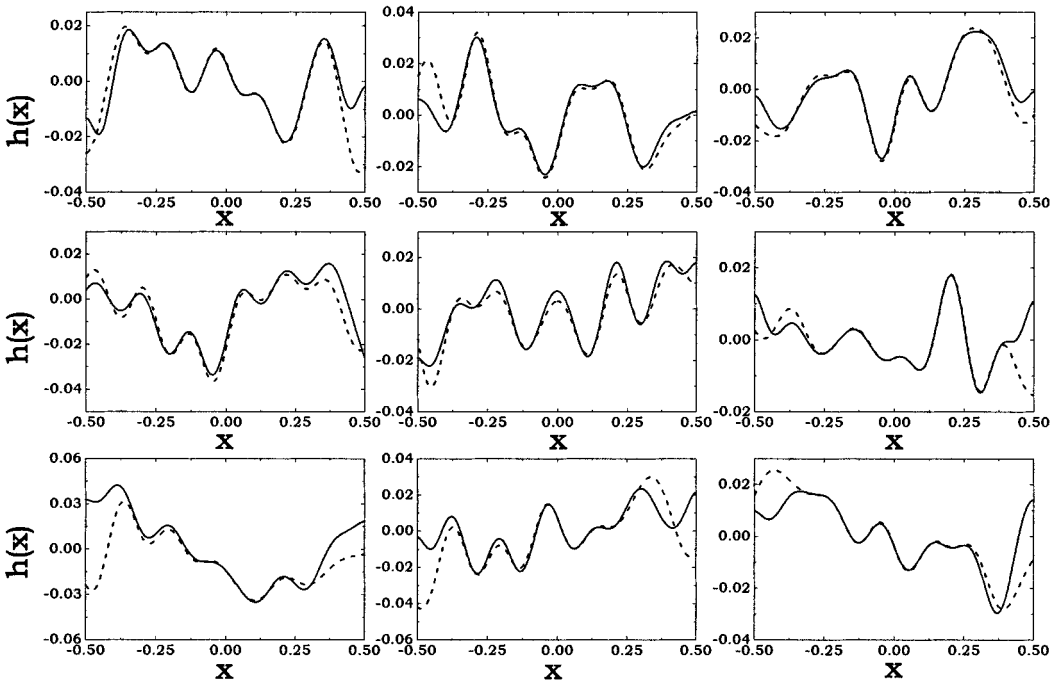

Fig. 8. Reconstruction of randomly chosen example profiles via the four-stage frequency-hopping strategy in Fig. 7. Spline parameters: $N_h = 12$, $\Delta_x = 1/12$, $x_{\min} = -0.5$, $x_{\max} = 0.5$; aperture parameters (nonphased cosine distribution (8)): $d = 0.8$, $z_A = 0.6$; observation points: $N_r = 10$, $z^r = 0.6$, $x_p^r = -0.5 + (p-1)/(N_r - 1)$, $p = 1, \ldots, N_r$; operating wavelengths: $N_\lambda = 4$, $\lambda_1 = 0.2$, $\lambda_2 = 0.1$, $\lambda_3 = 0.067$, $\lambda_4 = 0.05$. —— Actual profile; −−− Reconstruction.

these regions, corresponding to the aperture field tapering; the tapering is required to avoid numerical artifacts attributed to edge effects.

We performed a thorough calibration of the proposed inversion algorithm, by reconstructing a large number of randomly generated surface realizations with moderate roughness both in height and slope ($\lesssim 40^\circ$). Representative results are shown in Fig. 8. For all examples we used the four-stage frequency-hopping scheme as in Fig. 7. Again, except near the edge regions, the reconstructions are quite accurate. As a general comment, we found satisfactory reconstructions for problem parameters (roughness, permittivity, etc.) in the range of validity of the forward model summarized in Section III-B.

We also investigated the numerical stability of the algorithm with respect to errors in the reflected field simulated/measured data. In order to simulate the unavoidable measurement uncertainty, we added to the full-wave-computed reflected field data a uniformly distributed relative error. Furthermore, in order to roughly simulate the effect of possible clutter sources neglected in the model, such as the incoherent scattering contribution from fine-scale roughness, we added a background noise with uniformly distributed amplitude and phase. Reconstruction results are shown in Fig. 9, with the problem parameters as in Fig. 3. As one can see, the reconstruction obtained from corrupted data with a relative error of $\pm 5\%$ in amplitude and $\pm 10^\circ$ in phase and a background noise of -20 dB, is not very different (apart from the edge regions) from that obtained using noise-free data, thus indicating the robustness of the proposed algorithm. Increasing the noise strength obviously results in a poorer reconstruction, especially in the edge regions whose *weaker* scattering contribution is more noise-sensitive. It is interesting to notice that even with a considerably stronger background noise (-10 dB), the reconstruction of the central region of the interface profile is still relatively accurate.

Concerning the convergence rate, in the above examples an average number of 20–30 conjugate gradient iterations per resolution stage was typically required, resulting in an overall computing time of ~ 1 min on a 500 MHz PC; no particular effort was made to optimize the numerical code.

V. Conclusions

We presented a new inversion algorithm for the reconstruction of moderately rough dielectric interfaces using spatially sampled (multifrequency) reflected field data. The proposed approach is based on a compact parameterization of the unknown interface profile in terms of quartic splines, whose unknown parameters are estimated by minimizing the *difference* between model-based and measured reflected field data. The approach uses a fast forward model based on quasi-ray Gaussian beams [11]. In order to avoid local minima, a frequency hopping multiresolution approach is used, exploiting reconstructions based only on longer wavelengths to provide initial guesses for higher resolution reconstructions.

The proposed algorithm was evaluated on noisy data generated from simulated profiles, illustrating that accurate and robust reconstructions can be obtained for moderate roughness (maximum slopes $\lesssim 40^\circ$), with reasonable computing times. Thus, extensions of the algorithmic approach to three-dimensional (3D) geometries should be feasible for realistic situations where sparse (multifrequency) data and limited computing resources are available and near real-time estimates are required.

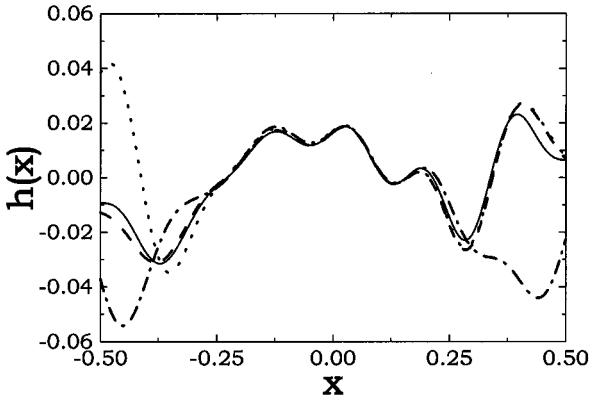

Fig. 9. Parameters as in Fig. 3. Reconstruction from noisy data via the four-stage frequency-hopping strategy in Fig. 7. —— Actual profile; – – – Reconstruction. (noise-free data); · · · · · · Reconstruction (relative error: $\pm 5\%$ in amplitude, $\pm 10^\circ$ in phase; background noise: -20 dB); — · — · — · — Reconstruction (relative error: $\pm 5\%$ in amplitude, $\pm 10^\circ$ in phase; background noise: -10 dB).

The approach presented in this paper is similar in spirit to that of [8], although based on a different forward solver and optimization schemes. In particular, our approach generalizes naturally to sparsely sampled data.

The surface estimation algorithm has been extended to time dependent (short pulse) GPR excitation [25] and has been incorporated into adaptive techniques for subsurface GPR image reconstruction of shallowly buried plastic mine-like targets in the presence of unknown rough air-soil interfaces [19]–[22]; preliminary outcomes seem encouraging. Extensions presently under investigation include generalization to fully 3D geometries.

REFERENCES

[1] T. Dogaru and L. Carin, "Time-domain sensing of targets buried under a rough air-ground interface," *IEEE Trans. Antennas Propagat.*, vol. 46, pp. 360–372, Mar. 1998.

[2] R. A. Weisenseel, W. C. Karl, D. A. Castañon, E. L. Miller, C. M. Rappaport, and C. A. DiMarzio, "Statistical fusion of GPR and EMI data," *Proc. SPIE, Detection and Remediation Technologies for Mines and Minelike Targets IV*, vol. 3710, pp. 1179–1187, 1999.

[3] T. Dogaru, L. Collins, and L. Carin, "Optimal time-domain detection of a deterministic target buried under a randomly rough interface," *IEEE Trans. Antennas Propagat.*, vol. 49, pp. 313–326, Mar. 2001.

[4] H. Zhan, C. M. Rappaport, M. El-Shenawee, and E. L. Miller, "Mine detection under rough ground surfaces using 2-D FDTD modeling and hypothesis testing," in *Proc. 2001 IEEE Antennas Propagat. Int. Symp.*, vol. 3, Boston, MA, July 8–13, 2001, p. 756.

[5] H. Feng, D. A. Castañon, W. C. Karl, and E. L. Miller, "GPR imaging approaches for buried plastic landmine detection," *Proc. SPIE, Detection and Remediation Technologies for Mines and Minelike Targets V*, vol. 4038, pp. 1485–1496, 2000.

[6] R. J. Wombell and J. A. DeSanto, "The reconstruction of shallow rough-surface profiles from scattered field data," *Inv. Probl.*, vol. 7, pp. L7–L12, 1991.

[7] ——, "Reconstruction of rough-surface profiles with the Kirchhoff approximation," *J. Opt. Soc. Amer. A*, vol. 8, no. 12, pp. 1892–1897, Dec. 1991.

[8] C. Ying and A. Noguchi, "Rough surface inverse scattering problem with Gaussian beam illumination," *IEICE Trans. Electron.*, vol. E77-C, pp. 1781–1785, Nov. 1994.

[9] K. Harada and A. Noguchi, "Reconstruction of two dimensional rough surface with Gaussian beam illumination," *IEICE Trans. Electron.*, vol. E79-C, no. 10, pp. 1345–1349, October 1996.

[10] A. Schatzberg and A. J. Devaney, "Rough surface inverse scattering with the Rytov approximation," *J. Opt. Soc. Amer. A*, vol. 10, no. 5, pp. 942–950, May 1993.

[11] V. Galdi, L. B. Felsen, and D. A. Castañon, "Quasi-ray Gaussian beam algorithm for time-harmonic two-dimensional scattering by moderately rough interfaces," *IEEE Trans. Antennas Propagat.*, vol. 49, pp. 1305–1314, Sept. 2001.

[12] J. J. Maciel and L. B. Felsen, "Systematic study of fields due to extended apertures by Gaussian beam discretization," *IEEE Trans. Antennas Propagat.*, vol. 37, pp. 884–892, July 1989.

[13] ——, "Gaussian beam analysis of propagation from an extended aperture distribution through dielectric layers, Part I—Plane layer," *IEEE Trans. Antennas Propagat.*, vol. 38, pp. 1607–1617, Oct. 1990.

[14] ——, "Gaussian beam analysis of propagation from an extended aperture distribution through dielectric layers, Part II—Circular cylindrical layer," *IEEE Trans. Antennas Propagat.*, vol. 38, pp. 1618–1624, Oct. 1990.

[15] L. L. Shumaker, *Spline Functions: Basic Theory*. New York, NY: Wiley, 1981.

[16] W. C. Chew and J. H. Lin, "A frequency-hopping approach for microwave imaging of large inhomogeneous bodies," *IEEE Microwave Guided Wave Lett.*, vol. 5, pp. 439–441, 1995.

[17] A. G. Tijhuis and K. Belkebir, "Using multiple frequency information in the iterative solution of a two-dimensional nonlinear inverse problem," in *Proc. Progress Electromagnetic Research Symp. (PIERS '96)*, Innsbruck, Austria, 1996.

[18] O. M. Bucci, L. Crocco, T. Isernia, and V. Pascazio, "Inverse scattering problems with multifrequency data: Reconstruction capabilities and solution strategies," *IEEE Trans. Geosci. Remote Sensing*, pt. 1, vol. 38, pp. 1749–1756, July 2000.

[19] V. Galdi, W. C. Karl, D. A. Castañon, and L. B. Felsen, "Approaches to underground imaging for object localization," *Proc. SPIE, Detection and Remediation Technologies for Mines and Minelike Targets VI*, vol. 4394, pp. 1082–1091, 2001.

[20] V. Galdi, L. B. Felsen, and D. A. Castañon, "Gaussian beam algorithm for rough surface underground imaging," in *Proc. 7th Int. Conf. Electromagnetics in Advanced Applications (ICEAA '01)*, Torino, Italy, Sept. 10–14, 2001, pp. 175–178.

[21] V. Galdi, H. Feng, D. A. Castañon, W. C. Karl, and L. B. Felsen, "Moderately rough surface underground imaging via short-pulse quasiray Gaussian beams," *IEEE Trans. Antennas Propagat.*, submitted for publication.

[22] ——, "Multifrequency subsurface sensing in the presence of a moderately rough air-soil interface via quasiray Gaussian beams," Radio Sci., Special Issue on 2001 URSI EMT Symp., to be published.

[23] O. M. Bucci and T. Isernia, "Electromagnetic inverse scattering: Retrievable information and measurement strategies," *Radio Sci.*, vol. 32, no. 6, pp. 2123–2137, Nov.–Dec. 1997.

[24] O. M. Bucci, L. Crocco, and T. Isernia, "Improving the reconstruction capabilities in inverse scattering problems by exploitation of close-proximity setups," *J. Opt. Soc. Amer. A*, vol. 16, pp. 1788–1798, July 1999.

[25] V. Galdi, J. Pavlovich, W. C. Karl, D. A. Castañon, and L. B. Felsen, "Moderately rough dielectric interface reconstruction via short-pulse quasiray Gaussian beams," *IEEE Trans. Antennas Propagat.*, submitted for publication.

[26] Y. Leviatan and A. Boag, "Analysis of electromagnetic scattering from dielectric cylinders using a multifilament current model," *IEEE Trans. Antennas Propagat.*, vol. AP-35, pp. 1119–1127, Oct. 1987.

[27] V. Galdi, L. B. Felsen, and D. A. Castañon, "Quasi-ray Gaussian beam algorithm for short-pulse two-dimensional scattering by moderately rough dielectric interfaces," *IEEE Trans. Antennas Propagat.*, vol. 49, pp. 1305–1314, Sept. 2001.

[28] B. Rao and L. Carin, "Beam-tracing-based inverse scattering for general aperture antennas," *J. Opt. Soc. Amer. A*, vol. 16, pp. 2219–2231, Sept. 1999.

[29] W. H. Press, S. A. Teukolsky, W. T. Vetterling, and B. P. Flannery, *Numerical Recipes in C: The Art of Scientific Computing*, 2nd ed. Cambridge, U.K.: Cambridge Univ. Press, 1992.

[30] E. Aarts and J. Korst, *Simulated Annealing and Boltzmann Machines: A Stochastic Approach to Combinatorial Optimization and Neural Computing*. New York: Wiley, 1989.

[31] K. F. Man, K. S. Tang, and S. Kwong, *Genetic Algorithms: Concepts and Designs*. New York: Springer, 1999.

[32] *Handbook of Global Optimization*, R. Horst and P. M. Pardalos, Eds., Kluwer, Dordrecht, The Netherlands, 1995.

[33] B. Z. Steinberg, H. Heyman, and L. B. Felsen, "Phase-space methods for radiation from large apertures," *Radio Sci.*, vol. 26, no. 1, pp. 219–227, Jan.–Feb. 1991.

Vincenzo Galdi (M'98) was born in Salerno, Italy, on July 28, 1970. He received the Laurea degree (summa cum laude) in electrical engineering and the Ph.D. degree in applied electromagnetics from the University of Salerno, Italy, in 1995 and 1999, respectively.

From April to December 1997, he held a visiting position with the Radio Frequency Division of the European Space Research & Technology Centre (ESTEC-ESA), Noordwijk, The Netherlands, where he was involved in developing CAD tools for microwave filters and phased-array antennas with coaxial excitation. In September 1999, he received a European Union postdoctoral fellowship through the University of Sannio, Benevento, Italy. In October 1999, he obtained a research associate position in the Department of Electrical and Computer Engineering at Boston University, Boston, MA, where he is currently working on wave-oriented imaging algorithms for landmine detection and classification. His research interests include analytical and numerical techniques for wave propagation in complex environments, path integrals and stochastic resonance.

Dr. Galdi is the recipient of a 2001 International Union of Radio Science (URSI) "Young Scientist Award." He is a member of Sigma Xi.

David A. Castañon (S'68-M'79-SM'98) received the B.S. degree in electrical engineering from Tulane University, New Orleans, LA, in 1971 and the Ph.D. degree in applied mathematics from the Massachusetts Institute of Technology (MIT), Cambridge, in 1976.

From 1976 to 1981, he was a Research Associate with the Laboratory for Information and Decision Systems at MIT. From 1982 to 1990, he was Senior and Chief Research Scientist at Alphatech, Inc., Burlington, MA. Since 1990, he has been a Professor in the Department of Electrical and Computer Engineering, Boston University, Boston, MA. His research interests include stochastic control and estimation, optimization and image processing.

Dr. Castañon served as a member of the Board of Governors of the IEEE Control Systems Society. He is also a member of the AMS, SIAM, and INFORMS.

Leopold B. Felsen (M'54–SM'55–F'62–LF'90) was born in Munich, Germany, on May 7, 1924. He emigrated to the United States in 1939 and served in the U.S. Army from 1943 to 1946. He received the B.E.E., M.E.E., and D.E.E. degrees from the Polytechnic Institute of Brooklyn, Brooklyn, NY, in 1948, 1950 and 1952, respectively.

After 1952, he remained with the Polytechnic (now Polytechnic University), gaining the position of University Professor in 1978. From 1974 to 1978, he was Dean of Engineering. In 1994, he resigned from the full-time Polytechnic faculty and was granted the status of University Professor Emeritus. He is now Professor of aerospace and mechanical engineering and Professor of electrical and computer Engineering at Boston University, Boston, MA (part-time). He is the author or coauthor of over 300 papers and of several books, including the classic *Radiation and Scattering of Waves* (Piscataway, NJ: IEEE Press, 1994). He is an associate editor of several professional journals and an editor of the *Wave Phenomena Series* (New York: Springer-Verlag). His research interests encompass wave propagation and diffraction in complex environments and in various disciplines, high-frequency asymptotic, and short-pulse techniques and phase-space methods with an emphasis on wave-oriented data processing and imaging.

Dr. Felsen is a member of Sigma Xi and a Fellow of the Optical Society of America and the Acoustical Society of America. He has held named Visiting Professorships and Fellowships at universities in the United States and abroad, including the Guggenheim in 1973 and the Humboldt Foundation Senior Scientist Award in 1981. In 1974 he was an IEEE/APS (Antennas and Propagation Society) Distinguished Lecturer. He was awarded the Balthasar van der Pol Gold Medal from the International Union of Radio Science (URSI) in 1975, an honorary doctorate from the Technical University of Denmark in 1979, the IEEE Heinrich Hertz Gold Medal for 1991, the APS Distinguished Achievement Award for 1998, the IEEE Third Millenium Medal in 2000 (nomination by APS), three Distinguished Faculty Alumnus Awards from Polytechnic University and an IEEE Centennial Medal in 1984. Also, awards have been bestowed on several papers authored or coauthored by him. In 1977 he was elected to the National Academy of Engineering. He has served on the APS Administrative Committee from 1963–1966 and as Vice Chairman and Chairman for both the United States (1966–1973) and the International (1978–1984) URSI Commission B.